Heliyon 10 (2024) e25887

Contents lists available at ScienceDirect

Heliyon

journal homepage: www.cell.com/heliyon

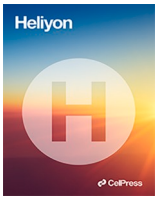

Research article

Langmuir monolayer studies of non-ionic surfactants and DOTMA for the design of ophthalmic niosomes

Axel Kattar [a,b], Emílio V. Lage [c], Matilde Casas [b,c], Angel Concheiro [a,b], Carmen Alvarez-Lorenzo [a,b,*]

[a] *Departamento de Farmacología, Farmacia y Tecnología Farmacéutica, I+D Farma Group (GI-1645), Facultad de Farmacia, and Health Research Institute of Santiago de Compostela (IDIS), Universidade de Santiago de Compostela, 15782, Santiago de Compostela, Spain*
[b] *Instituto de Materiales (iMATUS), Universidade de Santiago de Compostela, 15782, Santiago de Compostela, Spain*
[c] *Department of Physical Chemistry, Biomembranes Lab, Faculty of Pharmacy, Universidade de Santiago de Compostela, 15782, Santiago de Compostela, Spain*

ARTICLE INFO

Keywords:
Langmuir monolayer
Niosome
Cholesterol
Tween 60
DOTMA
π-A isotherm

ABSTRACT

The worldwide increase in diabetes entails a rise in associated diseases, with diabetic retinopathy on the forefront of the ocular complications. To overcome the challenges posed by ocular barriers, self-assembled nanocarriers have gathered increasing attention in recent years, with niosomes revealing themselves to be suitable for the delivery of a variety of drugs. This study investigated the mechanical properties of Langmuir monolayers comprising cholesterol, Tween 60, and 1,2-di-*O*-octadecenyl-3-trimethylammonium propane (DOTMA), both individually and in binary and ternary systems. The cholesterol monolayer was characterized by an L-shaped isotherm, reflecting two surface aggregation states. Tween 60 exhibited expanded conformation and progressive aggregation, transitioning through a phase change. The addition of cholesterol to Tween 60 resulted in a subtle reduction in surface compressional modulus. The compression isotherms highlighted the stabilizing effect of cholesterol on the monolayer, affecting the film's resistance to compression. The introduction of DOTMA in Tween 60 monolayers revealed concentration-dependent effects, where the compression resistance of the film was proportional to DOTMA concentration. Ternary systems of cholesterol, DOTMA and Tween 60 exhibited unique behavior, with DOTMA enhancing film stability and cholesterol modulating this effect. Temperature and subphase ionic strength variations further exacerbated the effects of DOTMA concentration. Brewster Angle Microscopy confirmed the absence of microdomains in the compressed monolayer, supporting the hypothesis of a monolayer collapse. Overall, the research provided valuable insights into the intricate interactions and mechanical behavior of these surfactant systems and the feasibility of obtaining cationic niosome-based drug delivery.

* Corresponding author. Departamento de Farmacología, Farmacia y Tecnología Farmacéutica, I+D Farma Group (GI-1645), Facultad de Farmacia, iMATUS, and Health Research Institute of Santiago de Compostela (IDIS), Universidade de Santiago de Compostela, 15782 Santiago de Compostela, Spain.

E-mail addresses: axel.kattar@usc.es (A. Kattar), emilio.lage@usc.es (E. V. Lage), matilde.casas@usc.es (M. Casas), angel.concheiro@usc.es (A. Concheiro), carmen.alvarez.lorenzo@usc.es (C. Alvarez-Lorenzo).

https://doi.org/10.1016/j.heliyon.2024.e25887
Received 18 January 2024; Accepted 5 February 2024
Available online 10 February 2024

1. Introduction

Ocular diseases strongly compromise people's quality of life. A common example is diabetic retinopathy that occurs in a third of diabetic patients, which may reach 700 million people by 2045 [1]. Pathological processes affecting the posterior segment of the eye prove especially hard to treat due to the many physiological barriers to overcome. Thus, there is an urgent need for nanocarriers that can be topically applied for an efficient delivery of the drug to the eye tissues or at least can reduce the need for frequent intravitreal injections [2,3].

Polymeric micelles [4] and vesicles such as liposomes [5] and niosomes [6] are self-assembled structures capable of encapsulating a range of molecules to carry and deliver their payload in various ocular sites. They are made by allowing amphiphilic molecules to arrange inside an aqueous medium, while either encapsulating hydrophobic drugs in the micelle core or vesicle bilayer, or encapsulating hydrophilic drugs in the vesicle core. These structures, and niosomes in particular, have been recently studied by our research group in terms of particle characterization, drug encapsulation and eye tissue permeation [7]. However, there are still gaps in the understanding of the physical chemistry of the aggregation and interaction between the molecules that make up the nanocarrier. Gathering this information is key to fully comprehend their behavior and optimize their composition, so as to improve the efficiency of the nanocarrier and hence the therapeutic action of the drug inside.

Langmuir monolayer studies have been previously demonstrated to be excellent tools for the rational design of a variety of self-assembled nanocarriers, such as cationically charged nonviral gene vectors made of didodecyldimethylammonium bromide (DDAB) [8], since the information on the interactions of the amphiphilic components at the air/water interface correlates with the interaction in the final bilayers/vesicles. Similarly, surface pressure–molecular area (π–A) isotherms have proved useful for inferring the stability of colloidal drug carriers and their interactions with drugs and cell membranes [9–12]. Information on niosomes is less abundant, and only very recently correlations between niosomes' properties and the excess free energy of mixed monolayers were described [13].

The aim of this study was to gain an insight into the molecular behavior and intermolecular interactions among the components present in neutral and cationic niosomes. The main hypothesis is that 1,2-di-*O*-octadecenyl-3-trimethylammonium propane (DOTMA), a common cationic surfactant (Fig. S1), plays a key role in the cohesion of the niosome. This has special relevance considering the possibility of cholesterol-mediated interactions with the voluminous hydrophilic group of polysorbate 60 (Tween 60), a common non-ionic surfactant used in niosome preparation. Indeed, the ability of cholesterol to form lipid rafts has been shown to oppose to the folding of the components to form small niosomes [13]. In the present work, the monolayers were made from Tween 60, cholesterol and different contents in DOTMA (Fig. S1). For pharmaceutical use and storage purposes, the effects of the ionic strength of the subphase and temperature on the behavior of the monolayers were also investigated.

2. Materials and methods

Materials. Polysorbate 60 (Tween 60, 1311.7 g/mol, HLB 14.9; Sigma Aldrich, Buchs, Switzerland), 1,2-di-*O*-octadecenyl-3-trimethylammonium propane (chloride salt) (DOTMA, 670.58 g/mol; Avanti, Alabaster, AL, USA), cholesterol (386.7 g/mol; Chemtrec, Madrid, Spain), dichloromethane (Fischer Scientific, Waltham, MA USA), and sodium bicarbonate (Merck, St Louis, MO, USA). Ultrapure water (resistivity >18.2 MΩ cm) was obtained by reverse osmosis (Milli-Q®, Millipore Ibérica, Madrid, Spain). Phosphate buffered saline (PBS) was made with 137 mM sodium chloride (Labkem, Barcelona, Spain), 10 mM disodium phosphate (Merck, St Louis, MO, USA), 1.8 mM potassium dihydrogen phosphate (Merck, Darmstadt, Germany) and 2.7 mM potassium chloride (Panreac, Castellar del Vallès, Spain) in distilled water.

Monolayer preparation. Prior to the beginning of the study, the trough was thoroughly cleaned with chloroform, and then with ethanol, along with both barriers and before each experiment, trough and barriers were cleaned with ethanol and rinsed twice with water. The surfactant solutions of Tween 60 and cholesterol at a fixed 100/42 mol/mol proportion, and DOTMA present at 5% and 10% the amount of Tween 60, were spread with a Hamilton microsyringe (Hamilton, USA) from dichloromethane solutions 0.2–0.4 mg/mL in 50–200 μL. After 10 min for solvent evaporation, film compression was registered plotting surface pressure values, measured with a platinum Wilhelmy plate (Biolin Scientific, Finland), against mean molecular area, rendering the π-A isotherms. Monolayers of different compositions were prepared and named according to the molar fractions displayed in Table 1.

***π*-A isotherm measurements.** Langmuir monolayers of Tween 60, cholesterol and DOTMA at the air/water interface were obtained on purified water (Milli-Q®; Millipore SAS, Merck, France) and PBS pH 7.4. The π-A isotherms were registered on a KSV-NIMA

Table 1
Composition of the different monomolecular films obtained in this work.

Monolayer code	Tween 60	Cholesterol	DOTMA	
	Mol fraction (%)	Mol fraction (%)	Mol fraction (%)	(mol % over Tween 60)
C	–	100	–	–
T	100	–	–	0
TD5	95.2	–	4.8	5.0
TD10	90.9	–	9.1	10.0
TC	70.4	29.6	–	0.0
TCD5	68.0	28.6	3.4	5.0
TCD10	65.8	27.6	6.6	10.0

KN 1006 (Biolin Scientific, Finland) Langmuir trough, with a working surface area of 783 cm^2 equipped with two barriers of poly (methylene oxide) (Delrin®) and placed into a safety cabinet to protect against dust and air convection. Surface pressure was measured with a precision of ±0.01 mN/m. The subphase temperature was 20 °C and 30 °C (±0.5 °C) maintained by a Julabo CD-200F (Julabo, Germany) heating circulator. In standard experiments, monolayers were compressed at a barrier speed of 10 mm/s. Each experiment was repeated at least three times with a reproducibility between the isotherms of ±0.2 $Å^2$/molecule.

Compressibility study. The surface compressional modulus (C_s^{-1}) or elasticity of a monolayer is a physical magnitude that positively correlate with the resistance of a film to compression [14], and was calculated according to **Equation 1**:

$$C_s^{-1} = -A\left(\frac{\partial \pi}{\partial A}\right)_T$$

where A is the mean molecular area for each point of the isotherm, and π is the surface pressure at that point and a given temperature [15,16]. Its value is known to rise with pressure, usually having a positive slope, since the closer molecules are to one another, the greater the resistance to further decreasing the distance between them will be, due to intermolecular repulsive forces [9]. A drop in its value reflects the existence of room for further compression that increases compressibility, usually standing for the collapse of the monolayer, which implies losing its 2D structure [17]. The compressibility modulus vs. surface pressure plots were obtained using the data analysis programme OriginLab 2019b. The raw plot line was smoothed by adjacent-averaging at every 5 points for noise reduction.

Brewster Angle Microscopy. BAM images of ternary systems were obtained using a Brewster Angle Microscope BAM 2 Plus (NFT, Göttingen, Germany) fitted with a 30 mW NdYAG laser emitting *p*-polarized light at a wavelength of 532 nm, and mounted directly on a NIMA 601BAM Langmuir trough (310 mL; NIMA, Coventry, UK) equipped with a PTFE (Teflon) barrier. The trough and the coupled microscope were placed on an antivibrational table (Halcyonics, Accurion GmbH, Germany) into a safety cabinet. The incident Brewster angle was set at 53.1° to reflect the laser on the air/water interface; this geometry ensures that there is no reflectivity of the *p*-polarized beam (R_p) on a pure water surface. Spreading a monolayer at the interface changes the refractive index of the medium and the Brewster angle, increasing the reflectivity and thus allowing to obtain an image from the *p*-polarized light. The reflected beam passes through a focal lens, into an analyzer at a known incident polarization angle and finishes its path into a CCD camera. Instead of the relative intensity (I), this camera measures the gray levels (GL), making up the image from those values.

3. Results and discussion

Effect of monolayer composition. The study was planned in an increasing order of complexity, evaluating first single components and the effects of cholesterol and DOTMA, separately, on Tween 60 monolayers. Pure DOTMA monolayers were not studied due to the limitations on the availability of the molecule and the unrealistic concentrations needed to obtain such monolayers. Then, the effect of cholesterol on Tween 60/DOTMA was assessed, obtaining ternary systems that mimic the niosome composition [8]. Compression isotherms and surface compressional modulus-surface pressure plots of each monolayer system were obtained. For the assessment of the effect of cholesterol on Tween 60 monolayers, π-A isotherms of pure Tween 60 (labelled as T) with pure cholesterol (C) were compared with a mixture of both components (TC) in the proportion stated in Table 1 π-A isotherms for pure cholesterol [18] are well described in the literature, while the behavior of Tween 60 solely [19] and combined with cholesterol has been less investigated. It should be noted that the relatively small size of our equipment forced us to use relatively high concentrations of the components in order to record changes in the region of interest, although this meant losing information on the behavior for large areas per molecule. Nevertheless, where considered relevant, isotherms were also recorded in dilute regimes.

Single component system. The L-shaped isotherm for cholesterol is explained by the two main conformations the molecules have at the air/water interface, and hence the two main surface aggregation states of the cholesterol monolayer (parallel to the interface and perpendicular to the interface) [20]. C_s^{-1} is depicted in Fig. 1. Polysorbate Tween 60 acquired an expanded conformation when spread on water, followed by a progressive aggregation, seen as a curve in the isotherm as surface pressure increased, and culminating in a phase transition or conformational change, as also seen for Tween 80 [21]. From a molecular point of view, the branched polar

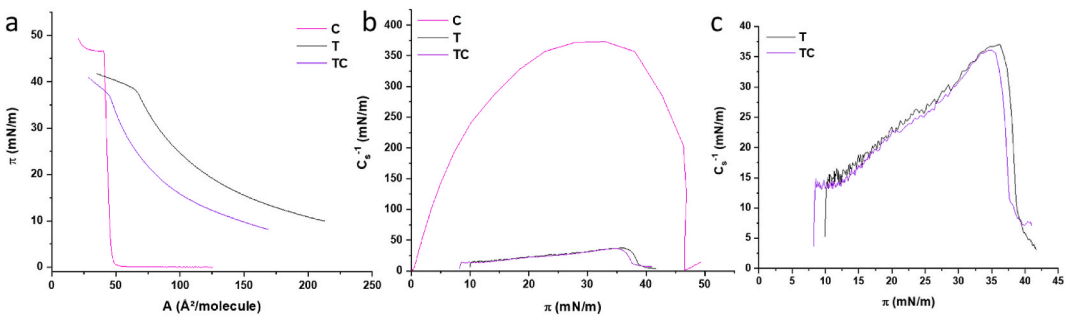

Fig. 1. Comparison of the surface pressure-area isotherm (a) and the surface compressional moduli (b) of pure cholesterol (C) and pure Tween 60 (T) monolayers and Tween 60/cholesterol mixture (TC), with zoom in the monolayers containing Tween 60 (c).

headgroups get closer to each other upon compression, and end up dehydrating if packed too tightly together [19], which might account for the slope change at the end of compression.

The high C_s^{-1} values recorded for cholesterol (max. at 373 mN/m) indicated a very condensed, rigid monolayer, mostly in a solid state of surface aggregation; the parabole-like shape (Fig. 1) accounted for the change of conformation cholesterol molecules perpendicular to the interface undergo upon compression [13,20]. Tween 60, on the contrary, formed an expanded, much more compressible monolayer (max. C_s^{-1} at 37 mN/m, 10 times less than the value for cholesterol) in a liquid-expanded (LE) aggregation state. This accounts for the fluidity of the niosomes, which are made of an average 68(±2)% Tween 60, which plays a key role as a property of the niosome membrane. A relatively fluid (LE state) vesicle membrane allows for the effective diffusion of its cargo, fundamental for drug delivery systems aiming to maximize the bioavailability of the therapeutic agent at the site of action. In terms of change with surface pressure, the C_s^{-1} of Tween 60 showed a steady rise as the monolayer was compressed, and then dropped at a surface pressure of 36.2 mN/m to progressively reach levels around or below those at the beginning of compression, tending to zero. This indicates the collapse of the monolayer, setting a limit of mean molecular area for Tween 60 molecules occupying a monolayer before a different molecular arrangement takes place. The difference in these results compared with those published previously where the lift-off takes places around 200 Å/molecule [13] would be explained by the difference in initial molecular packing arrangement at the interface due to the 3 times more number of molecules initially spread in our system.

Binary systems. To study the interaction between both components, mixed monolayers at a fixed composition (Table 1) were spread and compressed. A Tween 60:cholesterol 70:30 mol/mol ratio was chosen since previous experiments evidenced that this content in cholesterol was the most adequate to form stable niosomes with Tween 60 [7]. This is in good agreement with π-A isotherms recorded for other nanocarriers in which amphiphilic components (DDAB and oleic acid) to cholesterol 5:2 M ratio [8] and monopalmitoyl glycerol plus dicetylphosphate to cholesterol 6:4 and 6:2 M ratios [22] were found as the optimal to render stable structures in aqueous medium.

The π-A isotherm of TC (Fig. 1) indicated that there exists an interaction, since the presence of cholesterol in the Tween 60 monolayer in the chosen proportion caused both a change in the slope of the second region of the isotherm appearing at high pressure (in the interval 37–40 mN/m, in which the C_s^{-1} vs. π plot proves the film is collapsing) and a minor change in the shape of the isotherm below that point. As for the surface compressional modulus, the addition of cholesterol to the Tween 60 film yields lower C_s^{-1} values (Fig. 1), which means cholesterol enhances the compressibility of Tween 60 monolayer. However, this effect was weak as the curve for the Tween 60/cholesterol mixture was in close vicinity of that for pure Tween 60, revealing the influence of cholesterol on the mechanical properties of the polysorbate film to be small under these conditions.

The non-polar group of Tween 60 is a stearoyl chain, identical to that of stearic acid (SA). Therefore, comparing values such as collapse surface pressure (π_{col}) in known SA/cholesterol mixed monolayers [23] with those from Tween 60/cholesterol films may provide information on intermolecular interactions. Cholesterol slightly decreased film rigidity in Tween 60 monolayers (Table S1), as it does in SA films [23], as seen by the decrease of the collapse pressure of the monolayer, as expected from a less rigid film [24]. Even though SA and cholesterol do not form miscible monolayers, thus showing different π_{col} values without a linear correlation to cholesterol content [25], Tween 60 and cholesterol do mix at the air/water interface, as can be deduced from the fact there is a single collapse for the mixture. Cholesterol polycyclic ring may intercalate among acyl chains [25,26]. The maximum C_s^{-1} value of SA/cholesterol (70/30 mol%) monolayers was 500–600 mN/m; i.e., one order of magnitude greater than that of Tween 60/cholesterol films at the same proportion. Such a huge difference can be attributed to the different structure of the hydrophilic moieties of SA (a carboxyl group) and Tween 60, with a voluminous poly(ethylene oxide) (PEO) group leading to a branched tetrahydrofuran ring with more PEO chains (Fig. S1). This bulky headgroup gives Tween 60 its greater compressibility compared to fatty acids with the same structure in their non-polar region.

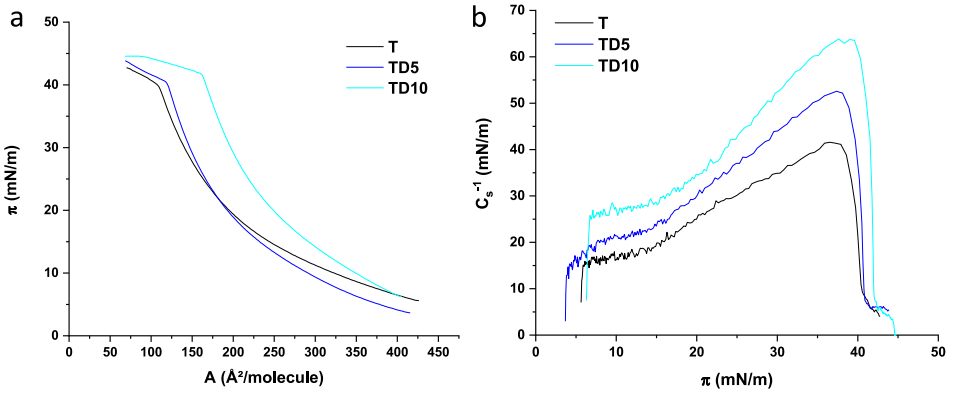

Fig. 2. π-A isotherms (a) and surface compressional moduli (b) of Tween 60 (T) monolayers incorporating 0%, 5% or 10% of DOTMA (coded as TD5 and TD10 respectively) at 20 °C.

Regarding the interaction between polar headgroups, the hydroxyl group of cholesterol, which lies close to the interface, can interact with the C═O bond in the ester group from polysorbate molecules' stearoyl chain, or the ester O atom in alpha position to the carbonyl bond of the same group. This interaction may occur via H-bonds between cholesterol hydroxyl H atom and the electron-rich O atom in the carbonyl bond and/or the aforementioned alpha O atom, as modelled through molecular dynamics [27]. This intermolecular interaction between polar moieties of both surfactants may increase lateral cohesion, leading to an improvement of shell stabilization in the niosomes [13].

Another proof of interaction given by the C_s^{-1} plot is how the final stage of decay of the modulus curve shows a different pattern than the one seen for pure Tween 60 films (coded as TC and T in Fig. 1, respectively). The existence of cholesterol among Tween 60 molecules and their possible interactions, as discussed above, may stabilize the monolayer at the last stage of collapse, changing the rate at which the film loses its monomolecular arrangement.

All analyzed parameters confirm that cholesterol, at the mole fraction used for the formation of niosomes described in a previous article [7], while not having a particularly large effect in terms of mechanical changes to Langmuir films, gives rise to interactions with Tween 60 at the monolayer which influence the stability of the film.

Secondly, the effect of DOTMA on Tween 60 monolayers was assessed by recording π-A isotherms (Fig. 2A) of binary mixtures where DOTMA content was 5% or 10% the amount of Tween 60 (see Table 1 for composition). Early stages of compression of Tween 60 monolayer showed initial pressures below 7 mN/m, with C_s^{-1} well below 12 mN/m (Fig. 2B) compatible with a gas (G) surface state of aggregation [28]. As surface pressure increased, the monolayer shifted to a mostly LE state for the rest of the isotherm, according to C_s^{-1} values (ca. 7–29 mN/m) [29,30].

DOTMA shifted the compression isotherm in two ways. Replacement of 4.8% of Tween 60 molecules by DOTMA molecules (TD5) changed the slope of the isotherm, particularly in the LE state but throughout the whole compression, possibly even changing the arrangement of molecules at the interface before compression (Fig. 3), all while retaining the shape of the isotherm of pure Tween 60, the majority component. From a molecular point of view, DOTMA molecules feature two hydrophobic C18:1 oleic chains that make it surface active, in spite of having a net charge (a trimethylammonium group) in its polar headgroup [18,31,32], so it was expected to remain at the interface along with Tween 60 molecules, probably intercalating and interacting with them, as shown later.

Further substitution of Tween 60 molecules by DOTMA molecules (TD10) yielded higher values of area per molecule, which follows the logic that DOTMA is more voluminous due to its structure with a double unsaturated fatty chain, hence taking up more space at the interface.

Interestingly, there was a correlation between the amount of DOTMA in the monolayer (0/5/10 mol%) and two important surface pressure values: the pressure at which the slope of the isotherm changes, due to a molecular rearrangement and/or a conformational change of the molecules at the interface (π_{trans}), and the collapse pressure (π_{col}). At surface pressure values higher than 22.3 mN/m, DOTMA causes an expansion of the monolayer, rendering higher values of area per molecule. This is consistent with the intercalation of unsaturated hydrocarbon chains, in this case in an amount proportional to DOTMA concentration, among saturated, single-chain stearic residues of Tween 60 molecules. The expanding effect of oleic chains has been reported in the literature for oleic acid/stearic acid [32] and saturated/unsaturated chain phospholipid interactions [33].

An interaction between both components was further evidenced by the concentration-dependent increase in the C_s^{-1} value with the proportion of DOTMA in the film at all π values (Fig. 2B). The surface pressure at which the peak of C_s^{-1} occurred, which is equivalent to say the point at which compressibility was the lowest throughout compression and the monolayer was most rigid, changed slightly with DOTMA proportion, but less than the surface compressional modulus values (Table S2).

Along with these differences, the C_s^{-1} values of the three compared T60/DOTMA systems indicated an increase in the resistance of the monolayer to compression as the amount of DOTMA increases. This increase in rigidity, apparently contrary to what is known about the aforementioned effect of hydrocarbon chain unsaturation, can be ascribed to the attractive interaction between DOTMA and Tween 60 polar headgroups. It can be hypothesized that the net positive charge on DOTMA quaternary ammonium

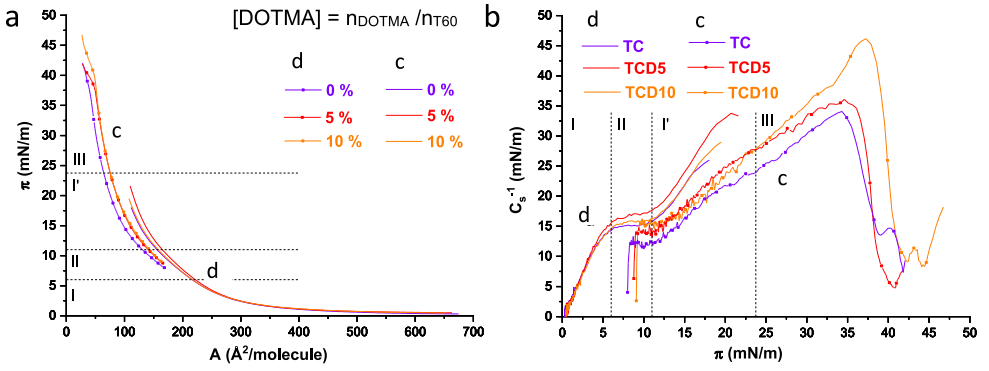

Fig. 3. π-A isotherms (a) and surface compressional moduli (b) of formulations TC, TCD5 and TCD10 at diluted (d) and concentrated (c) regimes at 20 °C.

(trimethylammonium) group (Fig. S1) can establish non-covalent electrostatic bonds with the more densely charged parts of the polysorbate branched headgroup, where the O atoms in the ester bond, in the adjacent ethylene oxide moiety and/or in the tetrahydrofuran ring are the most likely to participate in such interaction. The existence of these ion-dipole bonds, some orders of magnitude times stronger than London interactions taking place between non-polar chains [34], is a possible explanation for the condensing, rigidifying effect.

Ternary systems. Once the effect of both cholesterol and DOTMA as individual components on Tween 60 was assessed, monolayers made of the three components were evaluated. These monolayers were studied in two different concentrations: diluted (a) and concentrated (b) regimes in Fig. 3; where the higher concentration films contained twice as many molecules as the ones from the lower concentration. This duplicity of experiments for the ternary system, whose composition was set based on previous studies with niosomes [7], was necessary in order to investigate the molecular arrangement of these surfactants at a very wide range of surface pressure by obtaining isotherms as representative as possible.

The reason that π-A isotherms recorded in diluted (d) and concentrated (c) regimes did not overlap resides in the influence of the number of molecules spread onto the air/water interface before compression, which determined the surface area available for molecules to arrange within the film at the beginning of compression [35]. The isotherms from the diluted regime began with a gas-liquid expanded (G/LE) state [36,37] and molecules moving mostly freely at the interface, up to ca. 550 $Å^2$/molecule, when the interaction between molecules started raising surface pressure significantly. At as low a pressure value as 3 mN/m, the isotherm corresponding to TCD5 was above TC and TCD10 values and yielding a higher surface pressure (21.6 mN/m, versus 18.0 and 19.5 mN/m for 0 and 10% DOTMA, respectively) at the end.

C_s^{-1} values for the diluted regime reflected the distinct behavior of TCD5 monolayers (Fig. 3Ba). The increased pressure shown by the isotherms correlated with an increased modulus, which means TCD5 films are more resistant to compression due to a higher packing arrangement. A sigmoid shape was seen in the surface compressional modulus vs surface pressure plot (Fig. 3Ba), which featured a typical positive slope for the first part of compression (region I, Fig. 3), then gave rise to a plateau in compressibility in the range of 6–11 mN/m for all compositions (region II), only to continue rising at higher pressures. This is a confirmation of the plateau hinted in Fig. 1 for the simplest system, Tween 60/cholesterol (TC curve for π = 7–12 mN/m). Taking into account the ca. 29% of cholesterol present in the mixture and the surface behavior of both surfactants, the most logical conclusion seems to be that the forces that make molecules repel each other upon compression are cancelled out by the attractive forces that rise when cholesterol molecules shift conformation from parallel to the interface ('lying down' on it) to perpendicular to it ('standing up') [20]. This attractive pull takes place via London dispersion interactions between the cholesterol planar, hydrophobic steroidal structure and non-polar stearyl chains belonging to Tween 60, as happens with stearic acid and cholesterol [38,39]. As soon as all cholesterol has changed conformation, compression continues without any other new interactions, making the plot resume its positive slope (region I′ in Fig. 3).

Regarding the effect of DOTMA concentration, the presence of DOTMA raised monolayer rigidity (given by C_s^{-1} values) for all concentrations studied, although more at 5 mol% than 10 mol% (Fig. 3Ba), with certain exceptions for the concentrated regime (Fig. 3Bb). The effect of DOTMA concentration here is different to the findings shown above for the binary system. Given the novelty of the introduction of cholesterol in the Tween 60/DOTMA film, it hints at a possible cholesterol/DOTMA interaction and points at a predominance of the expanding effect of oleic chains, which are more numerous with greater DOTMA concentration, given the relatively large distance between polar headgroups for a proper interaction.

In the concentrated regime, the trend established for the diluted regime continued (region I′, Fig. 3) until the monolayer reached π = 23.7 mN/m, point at which the TCD10 film became less compressible than the TCD5 film (transition from region I' to III in Fig. 3). We ascribe this change to the fact that, if prior to this point the polar headgroups were not close enough to one another for the attractive electrostatic interactions to manifest themselves, hence leaving the system governed by the expanding effect of the oleic chains from DOTMA, at pressures higher than this the interaction between the surfactants in the monolayer is now governed by the polar headgroups, thus making the film more rigid.

Furthermore, Tween 60 has a voluminous, branched headgroup that makes the surfactant moderately hydrophilic (solubility ca. 100 g/L). The three polyether chains in this polar region of the surfactant, all in the subphase, are assumed to be highly hydrated and have a certain distance between each other. Upon compression beyond 24 mN/m, they start getting closer to each other, decreasing its overall effective volume and progressively dehydrating [40], which may facilitate the interactions of DOTMA trimethylammonium group, particularly with cholesterol (the electron-rich oxygen atom in cholesterol hydroxyl group). These attractive interactions, as well as the discussed Tween 60/DOTMA interaction, also ion-dipole in nature, make the monolayer adopt a tighter, more stable packing arrangement, becoming more resistant to compression, thus yielding higher C_s^{-1} values. This also leads to the conclusion that both cholesterol and DOTMA play a role in stabilizing the T60/DOTMA/cholesterol monolayer, and therefore the niosomes, making both components necessary at the same time.

The other important feature in region III seen in Fig. 3 is that, immediately after rising to a maximum compressibility, there was a dramatic, sudden fall in this property of the film. This was also observed as an evident change of slope in the pressure-area isotherms above ~40 mN/m (Fig. 3A), and it can be ascribed to a conformational change that leads to the collapse of the monolayer.

Collapse implies the loss of the monolayer's structure, after which molecules at the interface are left in a loosely packed arrangement, with plenty of free surface area, that allows further compression and approximation of the molecules to each other. The mechanism through which this phenomenon takes place can follow one out of these two routes: either the formation of a volume phase (multilayer formation), as seen in many lipids such as fatty acids [41], or surfactant desorption into the subphase. It is tempting to rule out the first option by the absence of a similar drop, in this case in surface pressure, in the compression isotherms [15]. In fact, upon analysis of the structure and solubility of the different chemical species present in the monolayer, as well of the interactions between them, could point at Tween 60, the most abundant and hydrophilic of the three components and the one with the largest polar

headgroup, abandoning the interface by solubilizing into the subphase. However, the pattern shown in the surface compressional modulus is similar to that shown in known cases of multilayer formation [42], suggesting this as the most probable mechanism of film collapse.

In any case, the collapse, given by the drop in C_s^{-1}, took place at higher values for the TCD10 monolayer (at 37.2 mN/m) than for TCD5 and TC monolayers (at 34.6 and 34.3 mN/m respectively), further accounting for the tighter packing of the film the higher the concentration of DOTMA for π values above ca. 24 mN/m, at which the vesicles are thought to be [13]. This is compatible with the data published by our group [7] on the good stability of niosomes with this exact composition after two months.

From the perspective of the effect of cholesterol, results show that, in spite of these well-established interactions and the stability of both the monolayers and the vesicles, the presence of cholesterol dampens the effect of DOTMA on Tween 60. This further indicates the existence of the cholesterol-DOTMA interactions. In term of mechanism, the intercalation of cholesterol polycyclic structure among hydrocarbon chains of Tween 60 and DOTMA may be responsible for this effect, similarly to what was hypothesized above for T60/cholesterol interactions. In fact, the drop in the maximum C_s^{-1} value due to cholesterol for the same T60/DOTMA proportion was greater the more DOTMA there was in the monolayer (Fig. 4): 24.47 mN/m for TCD10; 16.04 mN/m for TCD5; 0.90 mN/m for TC. Cholesterol therefore prevents monolayer packing in Tween 60/DOTMA systems proportionately to the amount of DOTMA, which gives more grounds to the probability of an interaction between DOTMA oleic chains and cholesterol.

The introduction of cholesterol in a T60/DOTMA system at a fixed proportion makes niosome-mimicking monolayers more compressible (Fig. 4). It is the same effect it has on pure T60, only to a much greater degree.

Effect of temperature. Isotherms from the compression of films with the three different DOTMA concentrations at the concentrated regime obtained at 20 °C and 30 °C (maximum temperature allowed at the interface for technical reasons related to the mechanical properties of the PTFE of the Langmuir trough) were compared in order to study whether the behavior of the monolayer at the air/water interface shown at room temperature is extensive to temperatures closer to that of the human eye (35 °C) [43], at which niosomes are intended to act.

The compression isotherms of these films at 20 °C and 30 °C displayed in Fig. 5A showed that the shape of the isotherms was the same at both temperatures, but that the behavior shown by the films with different amounts of DOTMA upon compression was completely different.

At 20 °C (Fig. 5A), DOTMA raised surface pressure throughout the whole compression and doubling the amount of DOTMA in the film implied greater surface pressure, if only at areas below ca. 60 $Å^2$/molecule. Along with the analysis of the elasticity of the monolayer, this reveals that the addition of DOTMA in the proportion range studied here raises the pressure at which the maximum compressibility (C_s^{-1}) is reached, from 34.6 mN/m at 5% to 37.2 mN/m at 10% the amount of Tween 60 (Fig. 5B), indicating an increased stability of the film, but remaining independent on DOTMA concentration at looser packing arrangements typical of greater values of molecular area. This implies that the influence of DOTMA concentration at this temperature is only affected via close range interactions, which take place at more densely packed molecular arrangements, hinting at polar group interactions as responsible for this effect.

At 30 °C, however, DOTMA caused a relevant decrease in surface pressure at any value of mean molecular area, in a proportional way to its concentration. To explore a quantitative approach to the influence of temperature in these films, the value for surface pressure yielded at the beginning of the compression of the film was analyzed, at an arbitrary value before the maximum elasticity point of the film for all systems, and right at the end of compression. Decreases in pressure of up to 10 mN/m were recorded for TCD10 at 30 °C compared to 20 °C (Table S4), which may be due to an increase in DOTMA solubility in the aqueous phase.

Effect of the subphase ionic strength. The ionic strength of the subphase influenced the monolayer behavior too (Fig. 6). While Tween 60/cholesterol binary systems had slightly lower modulus with increasing ionic strength of the subphase, the ternary systems showed higher modulus. This effect is expected as the ternary systems include the charged DOTMA, and goes in the same direction as

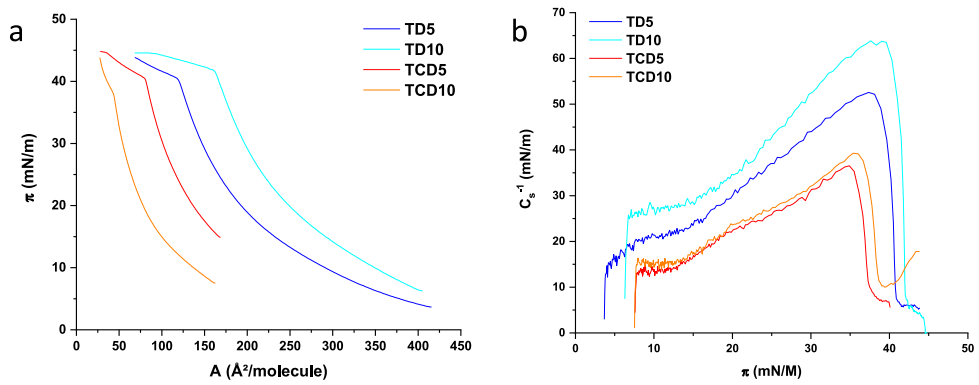

Fig. 4. π-A isotherms (a) and surface compressional moduli (b) of Tween 60 monolayers at 5% and 10% DOTMA with and without cholesterol at 20 °C.

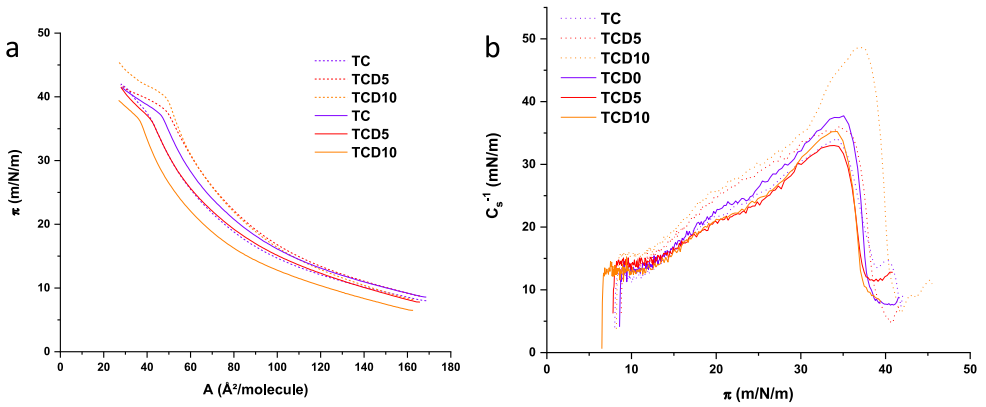

Fig. 5. π-A isotherms (a) and surface compressional moduli (b) of Tween 60/cholesterol/DOTMA monolayers at 20 °C and 30 °C. The dashed lines represent the monolayers at 20 °C and the solid lines represent the monolayers at 30 °C.

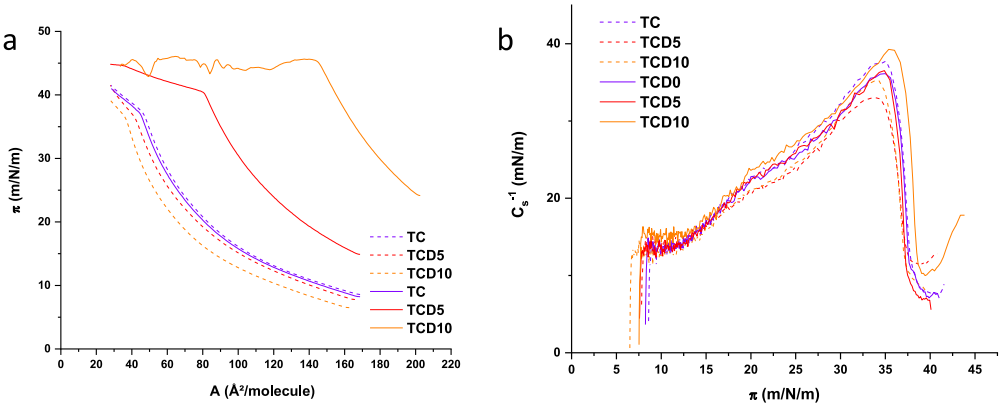

Fig. 6. π-A isotherms (a) and compressibility moduli (b) of Tween 60/cholesterol/DOTMA monolayers at 30 °C on water and PBS. The dashed lines represent the monolayers deposited onto pure water and the solid lines represent the monolayers deposited onto PBS.

the published data [44,45]. The ions present in the subphase interacting with the polar headgroup of DOTMA can lead to a salting out effect [46], increasing the effect of DOTMA at the interface. The concentration of salts of the PBS subphase as well as the cationic charge on the DOTMA are the main driving factors in the electrostatic effect.

Brewster Angle Microscopy. The BAM images were obtained by compressing a monolayer of TCD5 on a water surface. The images were taken at regular intervals, and while the available equipment did not permit taking video footage, the movement of the monolayer was clear starting at 80 $Å^2$/molecule. The resolution of the images is 96 dpi and there was no post processing applied. The camera quality did not allow for higher resolution, therefore the analysis of these image only permitted general conclusions. Furthermore, in images presented in Fig. 7 the monolayer is seen as the darkening of the image.

The BAM images in Fig. 7 show no presence of microdomains [47]. When compression happens and the spatial restrictions on the molecules increases, the only noticeable feature is a darkening of the image attributed to more reflection of the polarized light by the monolayer. This indicates an increase in density of the monolayer when compressed, and supports the previous compressibility study findings and the comparison with previously published data [48].

4. Conclusion

The role of small, increasing amounts of DOTMA in Langmuir monolayers of this surfactant along with Tween 60 (making up a little over two thirds of the film) and cholesterol as main components has been assessed by film compression and the analysis of their mechanical properties. DOTMA increases monolayer rigidity, given by the surface compressibility modulus, in a concentration-dependent way through interactions with both Tween 60 and cholesterol at the air/water interface, contributing and giving a

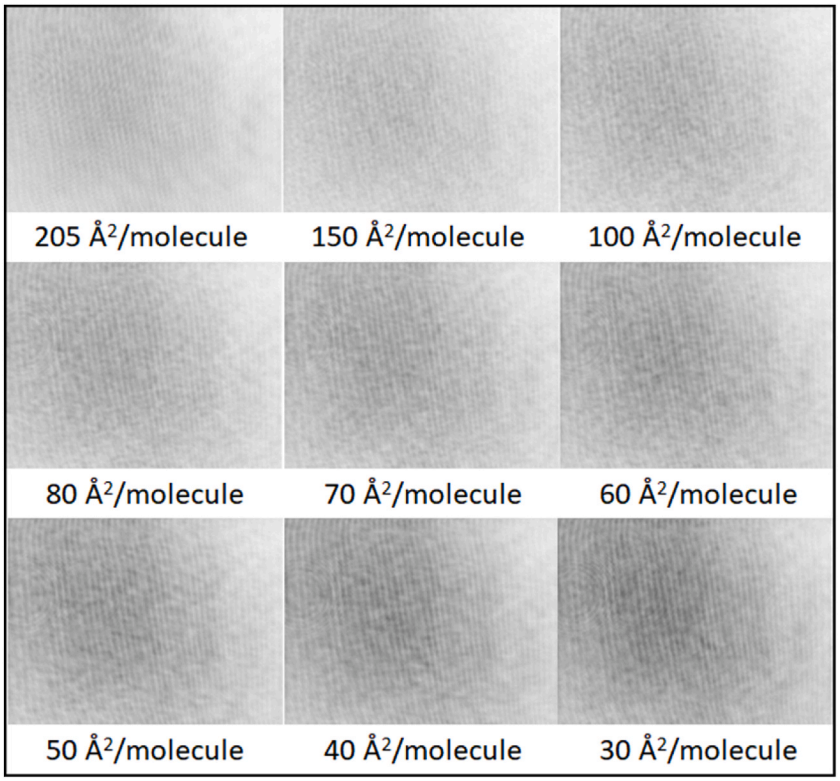

Fig. 7. BAM images of the compression of the TCD5 monolayer on PBS at 20 °C.

molecular explanation to the stability of the monolayer and of the vesicle.

The studies on these monolayers also probed the stability of niosomes before changes in physicochemical properties from storage conditions (water formulation, 20 °C) to administration conditions in the eye (electrolytic medium, closer to 30 °C), studying the influence of temperature and ionic strength in both environments. Results obtained at the air/water interface suggest that, as shown for the addition of DOTMA to the binary Tween 60/cholesterol system, film fluidity is increased at 30 °C. The films also show a tighter packing arrangement in PBS than in water, as pointed at by the much higher values of pressure at the beginning of compression. The behavior of these monolayers suggests an enhanced stability of the niosome in the eye environment due to the electrolytes present, coupled with an increased permeability that hinders undesired tightly packing arrangements which might negatively affect the diffusion of the drug meant to be delivered in the eye.

This work and the conclusions drawn from it intend to give further insight on how interface science, particularly the study of aggregation colloids in monolayers at the air/water interface, provides a very useful tool to study their conformation in the aggregate, the interactions between its components, and how gathering this information is key to the design and optimization of colloids for any given purpose, in this case the encapsulation and release of drugs into the eye.

Funding

This research was funded by the European Union's Horizon 2020 research and innovation program under the Marie Sklodowska-Curie Actions (grant agreement-No 813440). The work was also supported by MCIN/AEI/10.13039/501100011033 [PID 2020-113881RB-I00 to A.C. and C.A.-L.], Spain, Xunta de Galicia [ED431C 2020/17], and FEDER.

CRediT authorship contribution statement

Axel Kattar: Writing – review & editing, Writing – original draft, Validation, Software, Methodology, Investigation, Formal analysis, Data curation, Conceptualization. **Emílio V. Lage:** Writing – review & editing, Writing – original draft, Validation, Software, Methodology, Investigation, Formal analysis, Data curation, Conceptualization. **Matilde Casas:** Writing – review & editing, Supervision, Resources. **Angel Concheiro:** Writing – review & editing, Supervision, Resources, Project administration. **Carmen Alvarez-Lorenzo:** Writing – review & editing, Supervision, Resources, Project administration, Funding acquisition, Conceptualization.

Declaration of competing interest

The authors declare the following financial interests/personal relationships which may be considered as potential competing interests:

Axel Kattar reports financial support was provided by Horizon Europe. If there are other authors, they declare that they have no known competing financial interests or personal relationships that could have appeared to influence the work reported in this paper.

Acknowledgements

The authors thank Prof. Isabel Sández-Macho for helpful insights and review.

Appendix A. Supplementary data

Supplementary data to this article can be found online at https://doi.org/10.1016/j.heliyon.2024.e25887.

References

[1] Z.L. Teo, Y.C. Tham, M. Yu, M.L. Chee, T.H. Rim, N. Cheung, M.M. Bikbov, Y.X. Wang, Y. Tang, Y. Lu, I.Y. Wong, D.S.W. Ting, G.S.W. Tan, J.B. Jonas, C. Sabanayagam, T.Y. Wong, C.Y. Cheng, Global prevalence of diabetic retinopathy and projection of burden through 2045: systematic review and meta-analysis, Ophthalmology 128 (11) (2021) 1580–1591, https://doi.org/10.1016/j.ophtha.2021.04.027.

[2] R. Bisht, A. Mandal, J.K. Jaiswal, I.D. Rupentha, Nanocarrier mediated retinal drug delivery: overcoming ocular barriers to treat posterior eye diseases, WIREs Nanomed Nanobiotechnol (2017) e1473, https://doi.org/10.1002/wnan.1473.

[3] A. Kattar, A. Concheiro, C. Alvarez-Lorenzo, Diabetic eye: associated diseases, drugs in clinic, and role of self-assembled carriers in topical treatment, Expert Opin. Drug Deliv. 18 (2021) 1589–1607, https://doi.org/10.1080/17425247.2021.1953466.

[4] F. Alvarez-Rivera, D. Fernández-Villanueva, A. Concheiro, C. Alvarez-Lorenzo, α-Lipoic acid in soluplus ® polymeric nanomicelles for ocular treatment of diabetes-associated corneal diseases, J. Pharm. Sci. 105 (2016) 2855–2863, https://doi.org/10.1016/j.xphs.2016.03.006.

[5] X. Chen, J. Wu, X. Lin, X. Wu, X. Yu, B. Wang, W. Xu, Tacrolimus loaded cationic liposomes for dry eye treatment, Front. Pharmacol. 13 (2022) 1–16, https://doi.org/10.3389/fphar.2022.838168.

[6] N. Jain, A. Verma, N. Jain, Formulation and investigation of pilocarpine hydrochloride niosomal gels for the treatment of glaucoma: intraocular pressure measurement in white albino rabbits, Drug Deliv 27 (2020) 888–899, https://doi.org/10.1080/10717544.2020.1775726.

[7] A. Kattar, A. Quelle-Regaldie, L. Sánchez, A. Concheiro, C. Alvarez-Lorenzo, Formulation and characterization of epalrestat-loaded polysorbate 60 cationic niosomes for ocular delivery, Pharmaceutics 15 (2023) 1247, https://doi.org/10.3390/pharmaceutics15041247.

[8] Y. Jin, S. Wang, L. Tong, L. Du, Rational design of didodecyldimethylammonium bromide-based nanoassemblies for gene delivery, Colloids Surfaces B Biointerf 126 (2015) 257–264, https://doi.org/10.1016/j.colsurfb.2014.12.032.

[9] T.M. Nobre, F.J. Pavinatto, L. Caseli, A. Barros-Timmons, P. Dynarowicz-Łatka, O.N. Oliveira, Interactions of bioactive molecules & nanomaterials with Langmuir monolayers as cell membrane models, Thin Solid Films 593 (2015) 158–188, https://doi.org/10.1016/j.tsf.2015.09.047.

[10] M. Rojewska, W. Smułek, A. Grzywaczyk, E. Kaczorek, K. Prochaska, Study of interactions between saponin biosurfactant and model biological membranes: phospholipid monolayers and liposomes, Molecules 28 (2023), https://doi.org/10.3390/molecules28041965.

[11] A. Bahadur, S. Cabana-Montenegro, V.K. Aswal, E.V. Lage, I. Sandez-Macho, A. Concheiro, C. Alvarez-Lorenzo, P. Bahadur, NaCl-triggered self-assembly of hydrophilic poloxamine block copolymers, Int. J. Pharm. 494 (2015) 453–462, https://doi.org/10.1016/j.ijpharm.2015.08.058.

[12] N. Dib, A.L. Reviglio, L. Fernández, G. Morales, M. Santo, L. Otero, F. Alustiza, A.C. Liaudat, P. Bosch, M. Calderón, M. Martinelli, M. Strumia, Formation and characterization of Langmuir and Langmuir-Blodgett films of Newkome-type dendrons in presence and absence of a therapeutic compound, for the development of surface mediated drug delivery systems, J. Colloid Interf. Sci. 496 (2017) 243–253, https://doi.org/10.1016/j.jcis.2017.02.036.

[13] V.V. Arslanov, E.V. Ermakova, D.I. Krylov, O.O. Popova, On the relationship between the properties of planar structures of non-ionic surfactants and their vesicular analogues – niosomes, J. Colloid Interface Sci. 640 (2023) 281–295, https://doi.org/10.1016/j.jcis.2023.02.110.

[14] R.L. Cerro, Moving contact lines and Langmuir–blodgett film deposition, J. Colloid Interface Sci. 257 (2003) 276–283, https://doi.org/10.1016/S0021-9797(02)00009-7.

[15] K. Przykaza, K. Woźniak, M. Jurak, A.E. Wiącek, R. Mroczka, Properties of the Langmuir and Langmuir–blodgett monolayers of cholesterol-cyclosporine A on water and polymer support, Adsorption 25 (2019) 923–936, https://doi.org/10.1007/s10450-019-00117-2.

[16] J.F. Nagle, Area compressibility moduli of the monolayer leaflets of asymmetric bilayers from simulations, Biophys. J. 117 (2019) 1051–1056, https://doi.org/10.1016/j.bpj.2019.08.016.

[17] J.L. Fidalgo Rodriguez, L. Caseli, R. Torres Rodrigues, J. Miñones Conde, P. Dynarowicz-Latka, Phase transition beyond the monolayer collapse – the case of stearic acid spread at the air/water interface, Colloids Surfaces A Physicochem. Eng. Asp. 623 (2021) 126781, https://doi.org/10.1016/j.colsurfa.2021.126781.

[18] C. Hao, Q. Liu, Q. Li, J. Zhang, R. Sun, Thermodynamic and structural studies of DMPC and DSPC with DOTAP mixed monolayers at the air–water interface, Russ. J. Phys. Chem. A 90 (2016) 214–219, https://doi.org/10.1134/S0036024415120079.

[19] K. Szymczyk, A. Zdziennicka, B. Jańczuk, Adsorption and aggregation properties of some polysorbates at different temperatures, J. Solution Chem. 47 (2018) 1824–1840, https://doi.org/10.1007/s10953-018-0823-z.

[20] J.L. Fidalgo Rodriguez, L. Caseli, J. Minones Conde, P. Dynarowicz-Latka, New look for an old molecule – solid/solid phase transition in cholesterol monolayers, Chem. Phys. Lipids 225 (2019) 104819, https://doi.org/10.1016/j.chemphyslip.2019.104819.

[21] S. Singhal, C.C. Moser, M.A. Wheatley, Surfactant-stabilized microbubbles as ultrasound contrast agents: stability study of span 60 and tween 80 mixtures using a Langmuir trough, Langmuir 9 (1993) 2426–2429, https://doi.org/10.1021/la00033a027.

[22] J.S. Wilkhu, D. Ouyang, M.J. Kirchmeier, D.E. Anderson, Y. Perrie, Investigating the role of cholesterol in the formation of non-ionic surfactant based bilayer vesicles: thermal analysis and molecular dynamics, Int. J.Pharm. 461 (2014) 331–341, https://doi.org/10.1016/j.ijpharm.2013.11.063.

[23] H. Katarzyna, P. Wydro, The influence of fatty acids on model cholesterol/phospholipid membranes, Chem. Phys. Lipids 150 (2007) 66–81, https://doi.org/10.1016/j.chemphyslip.2007.06.213.

[24] A. Sarkar, K.A. Suresh, P. Kumar, N. Jayaraman, Strain rate and temperature dependence of collapse pressure in Langmuir monolayer of cholesteryl dimers, Thin Solid Films 735 (2021) 138900, https://doi.org/10.1016/j.tsf.2021.138900.

[25] R. Seoane, J. Miñones, O. Conde, J. Miñones, M. Casas, E. Iribarnegaray, Thermodynamic and brewster angle microscopy studies of fatty acid/cholesterol mixtures at the air/water interface, J. Phys. Chem. B 104 (2000) 7735–7744, https://doi.org/10.1021/jp001133+.

[26] J. Fantini, F.J. Barrantes, How cholesterol interacts with membrane proteins : an exploration of cholesterol-binding sites including CRAC, CARC, and tilted domains, Front. Physiol. 4 (2013) 1–9, https://doi.org/10.3389/fphys.2013.00031.

[27] A. Ritwiset, S. Krongsuk, J.R. Johns, Molecular structure and dynamical properties of niosome bilayers with and without cholesterol incorporation: a molecular dynamics simulation study, Appl. Surf. Sci. 380 (2016) 23–31, https://doi.org/10.1016/j.apsusc.2016.02.092.
[28] P. Toimil, G. Prieto, J. Miñones, F. Sarmiento, A comparative study of F-dppc/DPPC mixed monolayers. Influence of subphase temperature on F-DPPC and DPPC monolayers, Phys. Chem. Chem. Phys. 12 (2010) 13323–13332, https://doi.org/10.1039/c0cp00506a.
[29] J.T. Davies, E.K. Rideal, Interfacial Phenomena, second ed., Academic Press, New York, 1963.
[30] A.E. Anwander, R.P.J.S. Grant, T.M. Letcher, Interfacial Phenomena, J. Chem. Educ. 65 (1988) 608, https://doi.org/10.1021/ed065p608.
[31] D. Lu, D.G. Rhodes, Mixed composition films of spans and tween 80 at the air-water interface, Langmuir 16 (2000) 8107–8112, https://doi.org/10.1021/la000396s.
[32] J. Torrent-Burgués, Thermodynamic behaviour of mixed films of an unsaturated and a saturated polar lipid. (Oleic acid-stearic acid and popc-dppc), Colloids and Interfaces 2 (2018), https://doi.org/10.3390/colloids2020017.
[33] P. Wydro, K. Witkowska, The interactions between phosphatidylglycerol and phosphatidylethanolamines in model bacterial membranes. The effect of the acyl chain length and saturation, Colloids Surfaces B Biointerf 72 (2009) 32–39, https://doi.org/10.1016/j.colsurfb.2009.03.011.
[34] J.W. Steed, J.L. Atwood, Supramolecular Chemistry, second ed., John Wiley and Son, Hoboken, New Jersey, 2009.
[35] R. Francis, G. Louche, R.S. Duran, Effect of close packing of octadecyltriethoxysilane molecules on monolayer morphology at the air/water interface, Thin Solid Films 513 (2006) 347–355, https://doi.org/10.1016/j.tsf.2006.01.065.
[36] W.D. Harkins, T.F. Young, E. Boyd, The thermodynamics of films: energy and entropy of extension and spreading of insoluble monolayers, J. Chem. Phys. 8 (1940) 954–965, https://doi.org/10.1063/1.1750610.
[37] D.G. Dervichian, Changes of phase and transformations of higher order in monolayers, J. Chem. Phys. 7 (1939) 931–948, https://doi.org/10.1063/1.1750347.
[38] A. Wnętrzak, A. Chachaj-Brekiesz, M. Janikowska-Sagan, J.L. Fidalgo Rodriguez, J. Miñones Conde, P. Dynarowicz-Latka, Crucial role of the hydroxyl group orientation in Langmuir monolayers organization–the case of 7-hydroxycholesterol epimers, Colloids Surfaces A Physicochem. Eng. Asp. 563 (2019) 330–339, https://doi.org/10.1016/j.colsurfa.2018.12.025.
[39] S. Grimme, J. Antony, S. Ehrlich, H. Krieg, A consistent and accurate ab initio parametrization of density functional dispersion correction (DFT-D) for the 94 elements H-Pu, J. Chem. Phys. 132 (2010) 154104, https://doi.org/10.1063/1.3382344.
[40] J.L. Fidalgo Rodríguez, P. Dynarowicz-Latka, J. Miñones Conde, Structure of unsaturated fatty acids in 2D system, Colloids Surfaces B Biointerf 158 (2017) 634–642, https://doi.org/10.1016/j.colsurfb.2017.07.016.
[41] C. McFate, D. Ward, J. Olmsted, Organized collapse of fatty acid monolayers, Langmuir 9 (1993) 1036–1039, https://doi.org/10.1021/la00028a026.
[42] M.M. Lipp, K.Y.C. Lee, D.Y. Takamoto, J.A. Zasadzinski, A.J. Waring, Coexistence of buckled and flat monolayers, Phys. Rev. Lett. 81 (1998) 1650–1653, https://doi.org/10.1103/PhysRevLett.81.1650.
[43] J.A. Scott, The computation of temperature rises in the human eye induced by infrared radiation, Phys. Med. Biol. 33 (1988) 243–257, https://doi.org/10.1088/0031-9155/33/2/004.
[44] Y. Wang, G. Wen, S. Pispas, S. Yang, K. You, Effects of subphase pH, temperature and ionic strength on the aggregation behavior of PnBA-b-PAA at the air/water interface, J. Colloid Interface Sci. 512 (2018) 862–870, https://doi.org/10.1016/j.jcis.2017.11.002.
[45] M.M. Sacré, E.M. El Mashak, J.F. Tocanne, A monolayer (π,ΔV) study of the ionic properties of alanylphosphatidylglycerol: effects of pH and ions, Chem. Phys. Lipids 20 (1977) 305–318, https://doi.org/10.1016/0009-3084(77)90071-8.
[46] J.X. Yang, W.N. He, J.T. Xu, B.Y. Du, Z.Q. Fan, Influence of different inorganic salts on crystallization-driven morphological transformation of PCL-b-PEO micelles in aqueous solutions, Chinese J. Polym. Sci. English Ed. 32 (2014) 1128–1138, https://doi.org/10.1007/s10118-014-1512-z.
[47] A.C.T. Teixeira, A.C. Fernandes, A.R. Garcia, L.M. Ilharco, P. Brogueira, A.M.P.S. Gonçalves da Silva, Microdomains in mixed monolayers of oleanolic and stearic acids: thermodynamic study and BAM observation at the air-water interface and AFM and FTIR analysis of LB monolayers, Chem. Phys. Lipids 149 (2007) 1–13, https://doi.org/10.1016/j.chemphyslip.2007.05.004.
[48] M. Nieto-Suárez, N. Vila-Romeu, P. Dynarowicz-Latka, I. Prieto, The influence of inorganic ions on the properties of nonionic Langmuir monolayers, Colloids Surfaces A Physicochem. Eng. Asp. 249 (2004) 11–14, https://doi.org/10.1016/j.colsurfa.2004.08.040.